Percolation and epidemics in a two-dimensional small world

M. E. J. Newman
Santa Fe Institute, 1399 Hyde Park Road, Santa Fe, New Mexico 87501

I. Jensen
Department of Mathematics and Statistics, University of Melbourne, Parkville, VIC 3010, Australia

R. M. Ziff
Michigan Center for Theoretical Physics and Department of Chemical Engineering, University of Michigan, Ann Arbor, Michigan 48109-2136

(Received 12 September 2001; published 16 January 2002)

Percolation on two-dimensional small-world networks has been proposed as a model for the spread of plant diseases. In this paper we give an analytic solution of this model using a combination of generating function methods and high-order series expansion. Our solution gives accurate predictions for quantities such as the position of the percolation threshold and the typical size of disease outbreaks as a function of the density of ''shortcuts'' in the small-world network. Our results agree with scaling hypotheses and numerical simulations for the same model.

DOI: 10.1103/PhysRevE.65.021904 PACS number(s): 87.23.Ge, 05.40.−a, 05.70.Jk, 64.60.Fr

I. INTRODUCTION

The small-world model has been introduced by Watts and Strogatz [1] as a simple model of a social network—a network of friendships or acquaintances between individuals, for instance, or a network of physical contacts between people through which a disease spreads. The model consists of a regular lattice, typically a one-dimensional lattice with periodic boundary conditions although lattices of two or more dimensions have been studied as well, with a small number of ''shortcut'' bonds added between randomly chosen pairs of sites, with density ϕ per bond on the original regular lattice. The small-world model captures two specific features observed in real-world networks, namely (i) logarithmically short distances through the network between most pairs of individuals and (ii) high network clustering, meaning that two individuals are much more likely to be friends with one another if they have one or more other friends in common. The model turns out to be amenable to treatment using a variety of techniques drawn from statistical physics and has as a result received wide attention in the physics community [2–7].

The small-world model has some problems, however. In particular, it is built on a low-dimensional regular lattice, and there is little justification to be found in empirical studies of social networks for such an underlying structure. As recently pointed out by Warren *et al.* [8], however, there is one case in which the small-world model may be a fairly accurate representation of a real-world situation, and that is in the spread of plant diseases. Plant diseases spread through physical contacts between plants—immediate contagion, insect vectors, wind, and so forth—and these contacts form a ''social network'' among the plants in question. However, plants are sessile, and confined by and large to the two-dimensional plane of the Earth's surface. Disease spread as a result of short-range contact between plants is thus probably well represented as a transmission process on a simple two-dimensional lattice, and disease spread in which some portion of transmission is due to longer-range vectors such as wind or insects may be well represented by a small-world model built upon an underlying two-dimensional lattice. Because of this, as well as because of inherent mathematical interest, a number of recent papers have focused on two-dimensional small-world networks [8,10,11]. (It is possible also that the model could be used to represent forest wildfires, whose spread may be influenced by long-range contacts as well as local ones. There is some evidence that models with local contacts only do not mimic real fires well [9].)

In this paper we study bond percolation on two-dimensional (2D) small-world networks. Bond percolation is equivalent to the standard susceptible/infectious/recovered (SIR) model of disease spread [8,12], in which all individuals are initially susceptible to the disease, become infected (and hence infectious) with some probability per unit time if one of their neighbors is infectious, and recover again, becoming uninfectious and also immune, after a certain time in the infectious state. The equivalence of the SIR model to percolation is straightforward, with the percolation threshold mapping to the epidemic threshold of the disease in the SIR model, and cluster sizes mapping to the sizes of disease outbreaks which start with a single disease carrier. Using a combination of an exact generating function method with a high-order series expansion, we derive approximate analytic results for the position of the threshold and the mean outbreak and epidemic sizes as a function of the density of shortcuts in the 2D small-world network and the percolation probability, which is equivalent to disease transmission probability. As we demonstrate, our results are in excellent agreement with those from other studies using different methods, as well as with our own numerical simulations.

II. GENERATING FUNCTION FORMALISM

We study the two-dimensional small-world model built on the square lattice. The model is depicted in Fig. 1. We de-

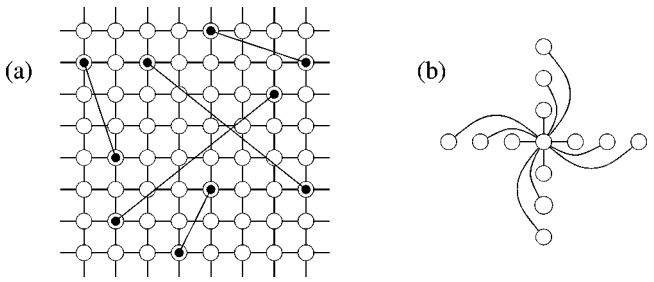

FIG. 1. (a) A two-dimensional small-world network built upon a square lattice with connection range $k=1$. (b) When $k>1$ the underlying lattice contains bonds beyond nearest-neighbor bonds along each principal axis out to range k, as shown here for $k=3$. This bond arrangement differs from that used in some other next-neighbor interaction models, but is conventional for the small-world model.

velop our generating function formalism for the general case of a d-dimensional square/cubic/hypercubic underlying lattice first, narrowing our scope to the two-dimensional case in Sec. III where we describe our series expansion calculations. For a d-dimensional lattice with bonds along the principal axes out to distance k [3], the underlying lattice has $dL^d k$ bonds on it, where L is the system dimension, and shortcuts are added with probability ϕ per underlying bond, for a total of $dL^d k\phi$ shortcuts. Then all bonds, including the shortcut bonds, are occupied with probability p, or not with probability $1-p$, and we construct the percolation clusters of sites connected by the occupied bonds.

The generating function part of our calculation follows the method of Moore and Newman [13]. We define a probability generating function $H(z)$ thus:

$$H(z)=\sum_{n=1}^{\infty} P(n)z^n, \tag{1}$$

where $P(n)$ is the probability that a randomly chosen site in our small-world network belongs to a connected cluster of n sites other than the system-spanning cluster. Note that if the probability distribution $P(n)$ is properly normalized, then $H(1)=1$ below the transition and $H(1)=1-S$ above the transition where S is the fraction of the system occupied by the system-spanning cluster.

We also define $P_0(n)$ to be the probability that a randomly chosen site belongs to a cluster of n sites on the underlying lattice. The complete cluster on the small-world network is composed of a set of such underlying clusters, joined together by occupied shortcut bonds. If we denote by $P(m|n)$ the probability that an underlying cluster of n sites has exactly m shortcuts emanating from it, then the generating function $H(z)$ can be written self-consistently as [13]

$$H(z)=\sum_{n=1}^{\infty} P_0(n)z^n \sum_m P(m|n)[H(z)]^m. \tag{2}$$

(The derivation of this equation assumes that all clusters other than the percolating cluster, if there is one, contain no closed loops other than those on the underlying lattice, i.e., there are no loops involving shortcut bonds. This is only strictly true in the limit of infinite system size, and hence our results will only be exact in this limit.)

There are a total of $2dL^d k\phi p$ ends of occupied shortcuts in the model, and since all ends are uniformly distributed over the lattice the probability that any end lands in a given cluster of size n is just n/L^d for large L. Thus $P(m|n)$ is given by the binomial distribution

$$P(m|n)=\binom{2dL^d k\phi p}{m}\left[\frac{n}{L^d}\right]^m\left[1-\frac{n}{L^d}\right]^{2dL^d k\phi p-m}. \tag{3}$$

Substituting into Eq. (2) and performing the sum over m, this gives

$$\begin{aligned} H(z)&=\sum_n P_0(n)z^n\left[1+(H(z)-1)\frac{n}{L^d}\right]^{2dL^d k\phi p} \\ &=\sum_n P_0(n)[ze^{2dk\phi p(H(z)-1)}]^n, \end{aligned} \tag{4}$$

where the last equality holds in the limit of large L. If we define the additional generating function

$$H_0(z)=\sum_n P_0(n)z^n, \tag{5}$$

which is the probability generating function for the sizes of clusters for ordinary bond percolation on the underlying lattice, then Eq. (4) can be written in the form

$$H(z)=H_0(ze^{2dk\phi p(H(z)-1)}). \tag{6}$$

This gives a self-consistency condition from which we can evaluate $H(z)$, and hence we can evaluate the probabilities $P(n)$ for cluster sizes in the small-world model.

In fact, it is rarely possible to solve Eq. (6) for $H(z)$ in closed form (although evaluation by numerical iteration is often feasible), but we can derive closed-form expressions for other quantities of interest. In particular, the average size of the cluster to which a randomly chosen site belongs is given by

$$\langle n\rangle=\sum_n nP(n)=H'(1)=H_0'(1)[1+2dk\phi pH'(1)], \tag{7}$$

or, rearranging,

$$\langle n\rangle=\frac{H_0'(1)}{1-2dk\phi pH_0'(1)}. \tag{8}$$

This quantity diverges when

$$2dk\phi pH_0'(1)=1, \tag{9}$$

or equivalently when

$$\phi = \frac{1}{2dkpH_0'(1)}, \tag{10}$$

and this point marks the phase transition at which a giant cluster scaling as a power of the system size first forms. Another way of looking at this result is to note that $H_0'(1) = \langle n_0 \rangle$, the average cluster size on the underlying lattice. Thus percolation takes place when

$$2dk\phi p = \frac{1}{\langle n_0 \rangle}. \tag{11}$$

The quantity on the left-hand side of this equation is the average density of the ends of occupied shortcut bonds on the lattice (see Sec. IV), and thus percolation takes place when there is on average exactly one end of an occupied shortcut bond per cluster on the underlying lattice. This is reminiscent of the phase transition in an Erdős-Rényi random graph, which occurs at the point where each vertex in the graph is attached to exactly one edge on average [14].

Above the phase transition $S = 1 - H(1)$ is the size of the giant cluster. Setting $z = 1$ in Eq. (6) we find that S is a solution of

$$S = 1 - H_0(e^{-2dk\phi pS}), \tag{12}$$

which can be solved by numerical iteration starting from a suitable initial value of S. An expression similar to Eq. (8) for the average size of nonpercolating clusters above the transition can also be derived. See, for example, Ref. [15].

III. SERIES EXPANSIONS

In the one-dimensional case studied in Ref. [13], the calculation of the generating function $H_0(z)$ is trivial—it is equivalent to solving the problem of bond percolation in one dimension. In the present case, however, we are interested primarily in the two-dimensional small-world model, and calculating H_0 is much harder; no exact solution has ever been given for the distribution of cluster sizes for bond percolation on the square lattice. Instead therefore we turn to series expansion to calculate H_0 approximately.

$H_0(z)$ for the two-dimensional case can be written as

$$H_0(z) = \sum_{stn} n z^n p^s (1-p)^t g_{stn}, \tag{13}$$

where g_{stn} is the number of different possible clusters on a square lattice which have s occupied bonds, t unoccupied bonds around their perimeter, and n sites. If we can calculate g_{stn} up to some finite order then we can calculate an approximation to $H_0(z)$ also. Unfortunately, because g_{stn} depends separately on three different indices, it is prohibitively memory intensive to calculate on a computer up to high order. We note, however, that we only need H_0 as a function of p and z, and not of $1-p$ separately, so we can collect terms in p and rewrite the generating function as

$$H_0(z) = \sum_{m=0}^{\infty} p^m Q_m(z), \tag{14}$$

where the quantities $Q_m(z)$ are finite polynomials in z which are, it is not hard to show, of order z^{m+1}. Calculating these polynomials is considerably more economical than calculating the entire set of g_{stn}. We have calculated them up to order $m = 31$ using the finite-lattice method [16], in which a generating function for the infinite lattice is built up by combining generating functions for the same problem on finite lattices. The finite lattices used in this case were rectangles of $h \times l$ sites and the quantity we consider is the fundamental generating function for the cluster density

$$G(z,p) = \sum_{stn} z^n p^s (1-p)^t g_{stn}, \tag{15}$$

which, it can be shown, is given by the linear combination

$$G(z,p) = \sum_{hl} w_{hl} G_{hl}(z,p), \tag{16}$$

where w_{hl} are constant weights that are independent of both z and p, and $G_{hl}(z,p)$ is the generating function for connected clusters (bond animals) which span an $h \times l$ rectangle both from left to right and from top to bottom.

Due to the symmetry of the square lattice, the weight factor w_{hl} is simply

$$w_{hl} = \begin{cases} 0 & \text{for } l < h \\ 1 & \text{for } l = h \\ 2 & \text{for } l > h. \end{cases} \tag{17}$$

The individual generating functions $G_{hl}(z,p)$ for the finite lattices are calculated using a transfer matrix method, with generating functions for all rectangles of a given height h being evaluated in a single calculation. The algorithm we use is based on that of Conway [17] with enhancements similar to those used by Jensen [18] for the enumeration of site animals on the square lattice [19]. Since clusters spanning a rectangle of $h \times l$ sites contain at least $h + l - 2$ bonds, we must calculate $G_{hl}(z,p)$ for all $h \leqslant (m+1)/2$ and $h \leqslant l \leqslant m - h + 2$ in order to derive a series expansion for $G(z,p)$ correct to order m in p. For the order $m = 31$ calculation described here the maximal value of h required was 16.

Once $G(z,p)$ is calculated, the polynomials $Q_m(z)$ are easily extracted by collecting terms in p. [Alternatively, one could write $H_0(z) = z\partial G/\partial z$, although doing so offers no operational advantage in the present case.] In Table I we list the values of $Q_m(z)$ for m up to 10; the complete set of polynomials up to $m = 31$ is available from the authors on request. We notice that since $H_0(1) = 1$ for all $p < p_c$, as it must given that the probability distribution it generates is properly normalized, it must be the case that

$$Q_m(1) = \begin{cases} 1 & \text{for } m = 0 \\ 0 & \text{for } m \geqslant 1. \end{cases} \tag{18}$$

TABLE I. The values of the polynomials $Q_m(z)$ up to $m=10$.

m	$Q_m(z)$
0	z
1	$4z^2-4z$
2	$18z^3-24z^2+6z$
3	$88z^4-144z^3+60z^2-4z$
4	$435z^5-860z^4+504z^3-80z^2+z$
5	$2184z^6-5020z^5+3784z^4-1008z^3+60z^2$
6	$11018z^7-28932z^6+26550z^5-9872z^4+1260z^3-24z^2$
7	$55888z^8-164668z^7+177972z^6-85100z^5+16912z^4-1008z^3+4z^2$
8	$284229z^9-928840z^8+1153698z^7-673836z^6+184125z^5-19880z^4+504z^3$
9	$1448800z^{10}-5197176z^9+7291488z^8-5030312z^7+1754424z^6-283320z^5+16240z^4-144z^3$
10	$7396290z^{11}-28890160z^{10}+45155952z^9-35926720z^8+15278872z^7-3323088z^6+317940z^5-9104z^4+18z^3$

It can easily be verified that this is true for the orders given in Table I. This implies that H_0 will be correctly normalized even if we truncate its series at finite order in p, as we do here. This makes our calculations a little easier.

In order to calculate the average cluster size (8) and position of the phase transition (10) in our small-world model, we need to evaluate the quantity $H_0'(1)$, which is given by

$$H_0'(1)=\sum_{m=0}^{\infty} p^m Q_m'(1). \tag{19}$$

The quantities $Q_m'(1)$ are just numbers—their values up to $m=31$ are given in Table II—so that this expression is a simple power series in p. If we make use of our results for m up to 31 to evaluate this quantity directly, we can calculate the behavior of the 2D small-world model using the results of Sec. II. However, we can do better than this.

Since $H_0'(1)$ is the average size $\langle n_0\rangle$ of a cluster in ordinary bond percolation on the square lattice, we know that it must diverge at $p_c=\frac{1}{2}$, and that it does so as $(p_c-p)^{-\gamma}$, where γ is the mean cluster-size exponent for two-dimensional percolation which is equal to $\frac{43}{18}$. With this information we can construct a Padé approximant to $H_0'(1)$ [21,22]. Writing

$$H_0'(1)=A(p)\left[\frac{p_c-p}{p_c}\right]^{-\gamma}, \tag{20}$$

where $A(p)$ is assumed analytic near p_c, we construct a Padé approximant to the series for

TABLE II. The derivatives $Q_m'(1)$ for all orders up to $m=31$, which are also the coefficients of the series for the mean cluster size—see Eq. (19). Note that although the values for $Q_m'(1)$ appear initially to be positive and increasing roughly exponentially, this rule does not hold in general. The first negative value is at $m=22$, and the signs of $Q_m'(1)$ appear to alternate for $m>22$.

m	$Q_m'(1)$	m	$Q_m'(1)$
0	1	1	4
2	12	3	36
4	88	5	236
6	528	7	1392
8	2828	9	7608
10	14312	11	39348
12	69704	13	197620
14	318232	15	1013424
16	1278912	17	5362680
18	4418884	19	28221636
20	11543548	21	152533600
22	−20880672	23	903135760
24	−705437704	25	5680639336
26	−7577181144	27	37205966052
28	−66485042424	29	253460708032
30	−534464876516	31	1767651092388

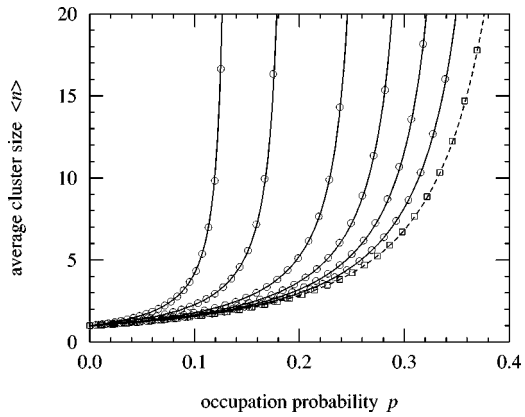

FIG. 2. The average of size in sites of the cluster to which a randomly chosen site belongs for bond percolation on a two-dimensional small-world network with $k=1$. The circles are simulation results for systems of 1024×1024 sites, calculated using the fast algorithm of Newman and Ziff [20], and the solid lines are the analytic result, Eq. (8). From left to right, the values of ϕ for each of the lines are 1.0, 0.5, 0.2, 0.1, 0.05, and 0.02. As ϕ diminishes the lines asymptote to the normal square lattice form which is indicated by the square symbols (simulation results) and the dotted line (series expansion/Padé approximant result).

$$A(p)=\left[\frac{p_c-p}{p_c}\right]^{\gamma}H_0'(1), \tag{21}$$

using our series for $H_0'(1)$. Then we use this approximant in Eq. (20) to give an expression for $H_0'(1)$ which agrees with our series expansion result to all available orders, and has a divergence of the expected kind at $p=\frac{1}{2}$. As is typically the case with Padé approximants, the best approximations are achieved with the highest order symmetric or near-symmetric approximants and using all available orders in our series expansion, we find the best results using a [15,15] approximant to $A(p)$ in Eq. (21). In Fig. 2 we show the resulting estimate for $\langle n_0\rangle=H_0'(1)$ (dotted line) as a function of p against numerical results for the average cluster size on an ordinary square lattice (squares). As the figure shows, the agreement is excellent.

Substituting our Padé approximant expression for $H_0'(1)$ into Eq. (8) we can now calculate average cluster size for the small-world model for any value of ϕ, and from Eq. (10) we can calculate the position of the phase transition. In Fig. 2 we show the results for $\langle n\rangle$ as a function of p along with numerical results for the same quantity from simulations of the model. In Fig. 3 we show the results for p_c plotted against numerical calculations [23]. In both cases, the agreement between analytic and numerical results is excellent. In the inset of Fig. 3 we show the results for p_c on logarithmic scales, along with the value calculated by using the series expansion for $H_0'(1)$ directly in Eq. (10) (dotted line). As the figure shows, the Padé approximate continues to be accurate to very low values of ϕ, where the direct series expansion fails.

IV. SCALING FORMS

As Ozana [11] has pointed out, there are two competing length scales present in percolation models on small-world networks. One is the characteristic length ξ of the small-world model itself which is given by $\xi=1/(2\phi kd)^{1/d}$, where d is the dimension of the underlying lattice (2 in the present case). This length is the typical linear dimension of the volume on the underlying lattice which contains the end of one shortcut on average. In other words $\xi^{-d}=2\phi kd$ is the density of the ends of shortcuts on the lattice. (In fact, one normally leaves the factor of 2 out of the definition of the characteristic length, but we include it since it makes the resulting formulas somewhat neater in our case.) In the current percolation model, only a fraction p of the shortcuts are occupied and thereby contribute to the behavior of the model—the unoccupied shortcuts can be ignored. Thus the appropriate characteristic length in our case is derived from the density of ends of occupied shortcuts, which was discussed in Sec. II. The correct expression is

$$\xi=\frac{1}{(2p\phi kd)^{1/d}}. \tag{22}$$

The other length scale is the correlation length or typical cluster dimension for the percolation clusters on the underlying lattice. Normally the latter is also denoted ξ, but to avoid confusion we follow the notation of Ref. [11] and here denote it ζ. Ozana has given a finite-size scaling theory for percolation on small-world networks which addresses the interaction of each of these length scales with the lattice dimension L. Our analytic calculations, however, treat the case of $L\to\infty$, for which a simpler scaling theory applies. In this

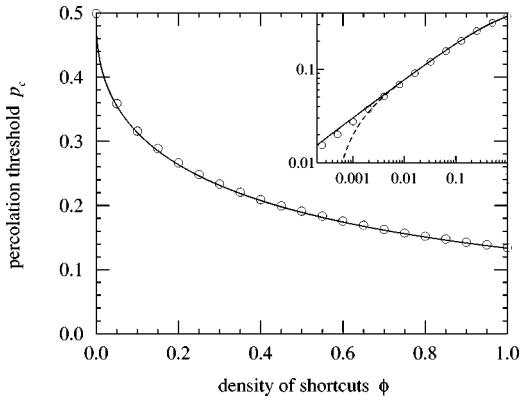

FIG. 3. The position of the percolation transition for the 2D small-world network as a function of the density ϕ of shortcuts. The points are simulation results, again using the algorithm of Ref. [20], and the lines are our analytic calculation using a Padé approximant. For the simulations, the value of p_c was taken to be the point at which the size of the largest cluster in the system has maximal gradient as a function of p. The slight difference between the numerical and analytic results appears to be a systematic error in the estimation of p_c from the numerical results (see Ref. [3] for a discussion of this point). Inset: the same comparison on logarithmic scales. In this case, the vertical axis measures $\frac{1}{2}-p_c$, which should go to zero with ϕ according to $\frac{1}{2}-p_c\sim\phi^{1/\gamma}$ where $\gamma=\frac{43}{18}$. [This can be deduced from Eq. (10), and is also shown in Ref. [8].] Again the solid line is the Padé approximant calculation, while the dotted line represents the value of p_c calculated directly from the series expansion without using a Padé approximant.

case, the only dimensionless combination of lengths is the ratio ζ/ξ, and any observable quantity $\mathcal{Q}$ must satisfy a scaling relation of the form

$$\mathcal{Q} \sim \zeta^{d\alpha} \xi^{-d\beta} f(\zeta/\xi), \tag{23}$$

where α and β are scaling exponents and $f(x)$ is a universal scaling function. This form applies when we are in the region where both ξ and ζ are much greater than the lattice constant, i.e., when shortcut density is low (the scaling region of the small-world model) and when we are close to the percolation transition on the normal square lattice.

We can rewrite Eq. (23) in a simpler form by making use of Eq. (22) and the fact that the typical cluster dimension ζ on the underlying lattice is related to typical cluster volume by $\zeta^d = \langle n_0 \rangle$ (assuming compact clusters). This then implies that

$$\mathcal{Q} \sim \langle n_0 \rangle^{\alpha} (p\phi kd)^{\beta} F(2p\phi kd\langle n_0 \rangle), \tag{24}$$

where $F(x)$ is another universal scaling function.

Consider, for example, the average cluster size $\langle n \rangle$ for the small-world model. Since we know this becomes equal to its normal square-lattice value $\langle n_0 \rangle$ when $\phi = 0$, we can immediately assume $\alpha = 1$, $\beta = 0$ and

$$\frac{\langle n \rangle}{\langle n_0 \rangle} = F(2p\phi kd\langle n_0 \rangle). \tag{25}$$

Thus a plot of $\langle n \rangle / \langle n_0 \rangle$ against the scaling variable $x \equiv 2p\phi kd\langle n_0 \rangle$ should yield a data collapse whose form follows the scaling function $F(x)$. In fact there is no need to make a scaling plot in this simple case. Comparison of Eq. (25) with Eq. (8), bearing in mind that $\langle n_0 \rangle = H_0'(1)$, reveals that $\langle n \rangle$ does indeed follow the expected scaling form with

$$F(x) = \frac{1}{1-x}. \tag{26}$$

The point $x = 1$, which is also the point at which the two length scales are equal $\xi = \zeta$, thus represents the percolation transition in this case. [This observation is equivalent to Eq. (11).]

A slightly less trivial example of the scaling form (24) is the scaling of the size S of the giant percolation cluster, Eq. (12). To deduce the leading terms in the scaling relation for S, we expand Eq. (12) close to the percolation transition in powers of S, to give

$$S = xS - \frac{[H_0'(1) + H_0''(1)]}{2[H_0'(1)]^2} x^2 S^2 + O(S^3). \tag{27}$$

Rearranging and keeping terms to leading order, we find

$$S \simeq \frac{2[H_0'(1)]^2}{[H_0'(1) + H_0''(1)]} \left[\frac{x-1}{x^2}\right] = 2\frac{\langle n_0 \rangle^2}{\langle n_0^2 \rangle} \left[\frac{x-1}{x^2}\right]. \tag{28}$$

If there is only one correlation length for percolation on the underlying lattice then $\langle n_0 \rangle^2 / \langle n_0^2 \rangle$ is homogeneous in it and hence constant in the critical region. Thus S scales as $S \sim (x-1)/x^2$ close to the transition, with the leading constant being zero below the transition and $O(1)$ above it.

V. CONCLUSIONS

We have presented analytic results for bond percolation in the two-dimensional small-world network model, which has been proposed as a simple model of the spread of plant diseases. Using a combination of generating function methods and series expansion, we have derived approximate but highly accurate expressions for quantities such as the position of the percolation transition in the model, the typical size of nonpercolating clusters, and the typical size of the percolating cluster. Our results are in excellent agreement with numerical simulations of the model. By judicious use of Padé approximants for the series expansions, the results can even be extended to very low shortcut densities, where a simple series expansion fails. The results are also in good agreement with the expected scaling forms for the model.

ACKNOWLEDGMENTS

The authors would like to thank Len Sander for helpful comments and Marek Ozana for providing an early preprint of Ref. [11]. This work was funded in part by the U.S. National Science Foundation and the Australian Research Council. Thanks are also due to the Australian Partnership for Advanced Computing for their generous allocation of computing resources.

[1] D.J. Watts and S.H. Strogatz, Nature (London) **393**, 440 (1998).
[2] M. Barthélémy and L.A.N. Amaral, Phys. Rev. Lett. **82**, 3180 (1999).
[3] M.E.J. Newman and D.J. Watts, Phys. Rev. E **60**, 7332 (1999).
[4] A. Barrat and M. Weigt, Eur. Phys. J. B **13**, 547 (2000).
[5] M.A. de Menezes, C.F. Moukarzel, and T.J.P. Penna, Europhys. Lett. **50**, 574 (2000).
[6] S.N. Dorogovtsev and J.F.F. Mendes, Europhys. Lett. **50**, 1 (2000).
[7] R.V. Kulkarni, E. Almaas, and D. Stroud, Phys. Rev. E **61**, 4268 (2000).
[8] C.P. Warren, L.M. Sander, and I.M. Sokolov, cond-mat/0106450.
[9] J.A.M.S. Duarte, in *Annual Reviews of Computational Physics*, edited by D. Stauffer (World Scientific, Singapore, 1997), Vol. 5.
[10] C.P. Warren, L.M. Sander, I.M. Sokolov, C. Simon, and J. Koopman (unpublished).
[11] M. Ozana, Europhys. Lett. **55**, 762 (2001).
[12] P. Grassberger, Math. Biosci. **63**, 157 (1983).
[13] C. Moore and M.E.J. Newman, Phys. Rev. E **62**, 7059 (2000).
[14] B. Bollobás, *Random Graphs* (Academic Press, New York, 1985).

[15] M.E.J. Newman, S.H. Strogatz, and D.J. Watts, Phys. Rev. E **64**, 026118 (2001).
[16] I.G. Enting, Nucl. Phys. B, Proc. Suppl. **47**, 180 (1996).
[17] A.R. Conway, J. Phys. A **28**, 335 (1995).
[18] I. Jensen, J. Stat. Phys. **102**, 865 (2001).
[19] Two practical differences between the algorithm we use and the algorithms used in previous calculations are that we use a transfer matrix with an intersection which cuts through the edges of the lattice rather than the vertices and we calculate a two parameter (z and p) generating function rather than just a one parameter (p) generating function. Most other aspects such as the encoding and transformations of the configurations of occupied and empty edges along the intersection and the rules for updating the associated generating functions are similar to earlier work.
[20] M.E.J. Newman and R.M. Ziff, Phys. Rev. Lett. **85**, 4104 (2000); Phys. Rev. E **64**, 016706 (2001).
[21] J.W. Essam and M.E. Fisher, J. Chem. Phys. **38**, 802 (1963).
[22] D.S. Gaunt and A.J. Guttmann, in *Phase Transitions and Critical Phenomena*, edited by C. Domb and M.S. Green (Academic Press, London, 1974), Vol. 3.
[23] In fact, the solid curves for $\langle n \rangle$ in Fig. 2 change little if one uses the series expansion, Eq. (19), directly in Eq. (8), rather than using the Padé approximant. As the inset of Fig. 3 shows, the difference between the series and the Padé approximant only becomes important for very small values of the shortcut density $\phi \lesssim 0.002$, and the curves in Fig. 2 do not reach such small values (except for the dotted $\phi = 0$ curve).